JOURNAL OF MOLECULAR RECOGNITION, VOL. **10**, 128–134 (1997)

Ligand Loading at the Surface of an Optical Biosensor and its Effect upon the Kinetics of Protein–Protein Interactions

P. R. Edwards,[1]* P. A. Lowe[1] and R. J. Leatherbarrow[2]*

[1] Affinity Sensors, East Bridge House, Saxon Way, Bar Hill, Cambridge, CB3 8SL, UK
[2] Biological Chemistry, Department of Chemistry, Imperial College of Science, Technology and Medicine, South Kensington, London SW7 2AY, UK

Optical biosensors are finding increasing use in the determination of kinetic and equilibrium constants for a variety of biomolecular interactions. Usually these biosensors require one biomolecule, the ligand, to be covalently attached to a hydrogel matrix which itself is bonded to the sensing surface. The ligands partner, the ligate, then binds from solution resulting in a measurable change in response which the instrument records as a function of time. Although in many cases, optical biosensors are used in order to obtain parameters that relate to interactions in solution, it is becoming clear that measurements involving the interaction of ligate with immobilized ligands on surfaces require careful experimental design. Here we report on how the density of ligand loading within the hydrogel matrix affects the measured interaction kinetics. It is found that crowding of ligand within this matrix results in a significant reduction in the measured association rate constant, with a corresponding effect in the calculated overall affinity. However, measurements at low ligand loadings show association rate constants that are comparable to those measured in solution. Clearly, where this comparison is required, it is important to perform measurements under such conditions. © 1997 John Wiley & Sons, Ltd.

J. Mol. Recogn. **10**, 128–134 (1997) No. of Figures: 10 No. of Tables: 0 No. of References: 24.

Keywords: **optical biosensor; IAsys; kinetics; protein–protein interactions**

Received 21 February 1996; accepted 17 July 1996.

Introduction

Molecular recognition between biomolecules is fundamental to an understanding of their biological function. Most conventional methods for characterizing biomolecular interactions provide only a measure of the dissociation equilibrium constant K_D (Stanley *et al*., 1983), the individual rate constants k_{ass} and k_{diss} (Equation 1) being difficult to determine by these methods.

$$G + L \underset{k_{diss}}{\overset{k_{ass}}{\rightleftharpoons}} GL \qquad K_D = \frac{k_{diss}}{k_{ass}} \tag{1}$$

Traditional methods generally rely upon the measurement of the concentration of free biomolecule in solution (i.e. the concentrations of G, the ligand or L, the ligate) after attainment of equilibrium. The detection of the free biomolecule often requires labelling (either with an enzyme or radioisotope), with possible deleterious effects on activity. In addition, bound and free biomolecules must typically be separated prior to measurement. The values of k_{ass} and k_{diss} define the interacting system more fully and allow, for example, the calculation of the lifetime of the GL complex. Despite the attraction of determining individual rates of association (k_{ass}) and dissociation (k_{diss}), there are few generally applicable techniques that supply such information.

Optical biosensors (Fägerstam *et al.*, 1990; Buckle *et al.*, 1993; Tiefenthaler, 1993) provide a convenient method for measuring individual rate constants in real-time by monitoring refractive index changes resulting at a surface when one biomolecule in solution binds to another covalently attached to a hydrogel such as a dextran matrix. High sensitivity, real-time monitoring and no requirement to label partners are advantages of optical biosensors over conventional methods.

The growing use of optical biosensors to probe kinetic parameters of interaction analysis has resulted in an ever increasing number of publications (Dubs *et al*., 1991; Malmborg *et al*., 1992; Kelley and O'Connell, 1993; Watts *et al*., 1994; George *et al*., 1995). However, the analysis of data generated from these biosensors is often less simple than data obtained from solution measurements, and the kinetics often differ from those expected in solution. (O'Shannessey *et al*., 1993; Zeder-Lutz *et al*., 1993; Felder *et al*., 1993; Corr *et al*., 1994; Edwards *et al*., 1995; George *et al*., 1995). Under the pseudo-first order conditions used for the biosensor experiments, association data should be described by a rate equation containing a single exponential function. However, at moderate to high ligate concentrations experimental biosensor data are often fitted better by an equation containing two exponential functions. Several reasons have been proposed to explain this unexpected result including heterogeneity of the immobilized ligand

* Correspondence to: P. R. Edwards and R. J. Leatherbarrow.

 CCC 0952–3499/97/030128–07 $17.50

(Zeder-Lutz *et al*., 1993; Mach *et al*., 1993; Bondeson *et al*., 1993), conformational changes of either ligand or ligate upon binding (Kelley and O'Connell 1993), and steric hindrance of binding within the surface matrix (Edwards *et al*., 1995). Yet another cause, in certain instances, may be multivalancy of ligand or ligate.

In this paper we present data generated using a commercially available resonant mirror biosensor (Buckle *et al*., 1994; Cush *et al*., 1994) that demonstrates a further factor which needs to be taken into account in experiments that use such instruments. We show that steric hindrance of ligate binding within the hydrogel matrix results in much reduced apparent association rate constants at high ligand loading. For our studies we have used the well-characterized protease/protease inhibitor system of chymotrypsin binding to chymotrypsin inhibitor-2.

Experimental

Materials

All chemicals used were of analytical reagent grade. Phosphate buffered saline (PBS) tablets and bovine α-chymotrypsin ($M_r = 25\,000$), were obtained from the Sigma Chemical Company (Poole, UK). Surfact-Amps® 20 was purchased from Pierce & Warriner (Chester, UK). Recombinant chymotrypsin inhibitor 2 (CI-2, $M_r = 9200$) was prepared as described by Jandu *et al.* (1990). An amine coupling kit [containing 1-ethyl-3-(3-dimethylaminopropyl) carbodiimide (EDC), N-hydroxysuccinimide (NHS) and 1 M ethanolamine, pH 8.5] and IAsys™ carboxymethyl dextran (CMD) cuvettes were from Affinity Sensors (Bar Hill, Cambridge, UK). PBS/T buffer was prepared by the addition of 0.05% v/v Surfact Amps® 20 to PBS buffer pH 7.4.

Operation of the optical biosensor system

Kinetic measurements were performed using the optical evanescent biosensor, IAsys™ (Affinity Sensors, Bar Hill, Cambridge, UK), following the procedures recommended by the manufacturer. The instrument detects changes in refractive index occurring within the evanescent field (a few hundred nanometers from the surface) when one biomolecule, the ligate, in solution binds to its partner, the ligand, immobilized onto the sensor surface. The immobilized ligand is attached to a surface-bound carboxymethyl dextran matrix extending 200–500 nm from the sensor surface. This negatively charged hydrophilic matrix helps to preserve the activity of the ligand and increases the surface area available for covalent attachment of the ligand. Ligand immobilization and ligate interactions can be followed in real-time with the instrument producing a plot of response, measured in arc seconds, against time. The IAsys instrument is based upon a cuvette system comprising of a sample well, with a working volume range of 50–200 μl, and the resonant mirror sensing surface. Temperature control was provided by a Peltier unit and a stirrer set at its maximum rate ensured the efficient delivery of the ligate to the sensor surface. A control experiment had previously shown that a binding rate independent of stir rate was achieved below this setting and thus mass-transport effects during experiments were minimized. All experiments using IAsys were performed at a cuvette temperature of 22°C with a solution volume of 200 μl.

Ligand immobilization to the CMD matrix

Ligands were covalently coupled to the CMD following activation of matrix carboxyl groups by the addition of a freshly prepared solution of EDC/NHS for 8 min. The EDC/NHS mixture was then replaced with PBS/T for 5 min and a pre-immobilization baseline response was established. Immobilization was initiated by the addition of the relevant ligand to the cuvette and allowing the interaction to proceed for 10 min. For the preparation of CMD surfaces containing differing ligand loadings chymotrypsin at concentrations of 2, 10, 50, 200, 500 and 2500 μg/ml prepared in 10 mM acetate pH 6.0 was immobilized in order to achieve a range of immobilization signals. This pH was found to give maximal electrostatic uptake (data not shown). After immobilization the ligand solutions were replaced by an ethanolamine wash for 2 min to react with residual NHS esters. The cuvette was finally washed with PBS/T to establish a post-immobilization response level. The amount of ligand immobilized can be calculated using the difference in the pre- and post-immobilization responses given that 1 ng protein mm^{-2} gives a response of 163 arc seconds on the IAsys instrument (Davies *et al*., 1994).

Monitoring the binding of ligate to immobilized ligand

CI-2 was dissolved in PBS/T to a concentration of 1240 nM. Before recording an interaction profile, the ligand-coupled cuvette was washed with the regeneration buffer (10 mM HCl) for 2 min to remove weakly bound ligand, and re-equilibrated in 180 μl PBS/T. To this solution, 20 μl of the appropriate ligate solution was added to give a final cuvette volume of 200 μl. Seven different CI-2 concentrations from 124 to 1.8 nM were used with a contact time of 10 min. After this period the cuvette contents were replaced with PBS/T buffer in order to monitor dissociation. Ligate was then fully removed with a 2-min 10-mM HCl wash followed by a 5-min PBS/T re-equilibration before the next binding cycle.

Kinetic analysis of interaction profiles

Data obtained from the biosensor for the interaction of CI-2 with immobilized chymotrypsin can be divided into two regions as shown in Figure 1. The first, often simplistically termed the 'association region', contains information on both the association and dissociation rate constants. The second region consists of dissociation events only (providing no rebinding occurs) and as such provides information about the dissociation rate constant. Analysis of data was performed as described previously (Edwards *et al*., 1995).

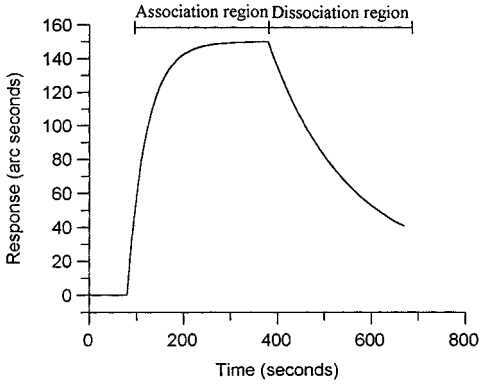

Figure 1. An interaction profile produced by the IAsys biosensor showing the association region obtained by the addition of ligate, and the dissociation region achieved by the replacement of ligate solution with buffer.

For biomolecular association of ligate with immobilized ligand at low ligate concentrations, the biosensor response, R (measured in arc seconds), is described by Equation 2.

$$R_t=(R_\infty-R_0)[1-\exp(-k_{on}t)]+R_0 \quad (2)$$

Here R_t is the response at time t, R_0 is the initial response, R_∞ is the maximal response, and k_{on} is the observed association rate constant.

At moderate to high ligate concentrations it is found that association data are poorly described by Equation (2), and it is necessary to fit the data to an equation containing two exponential terms (Equation 3).

$$R_t=A[1-\exp(-k_{on(1)}t)]+B[1-\exp(-k_{on(2)}t)]+R_0 \quad (3)$$

In this equation, the instrument response, R_t, varies with two apparent association rate constants ($k_{on(1)}$ and $k_{on(2)}$); the magnitudes, or extents, of the two phases are A and B, respectively, such that the total response, $R_\infty=R_0+A+B$ (Figure 2). We have previously shown that a major reason for this effect is steric hindrance of ligate binding within a hindered hydrogel surface matrix (Edwards *et al*., 1995), and the faster of the two rate constants should be used in order to derive association rate constants that are comparable to those obtained in solution.

The value of k_{on} varies with ligand concentration as described by Equation 4.

$$k_{on}=k_{diss}+k_{ass}[\mathrm{L}] \quad (4)$$

A plot of k_{on} against [L] allows the association constant, k_{ass}, to be determined from the slope and the dissociation constant, k_{diss}, from the intercept. However, the value of k_{diss} so obtained is often close to zero and inaccurately defined. Hence, k_{diss} is usually best measured by removing all the free ligate and monitoring directly the dissociation of the GL complex. Dissociation is observed as an exponential decay of the complex with time as described in Equation 5.

$$\mathrm{R}_t=R_0\exp(-k_{diss}t) \quad (5)$$

In this equation, the amount of complex at time t, R_t, is dependent upon the initial complex concentration, R_0, and the dissociation rate constant, k_{diss}. Given that the dissociation is a first-order process, the half-life of the GL complex can be determined from Equation 6

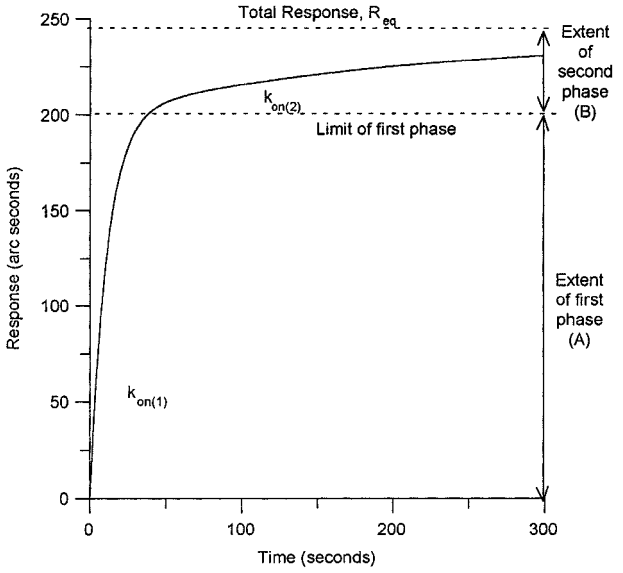

Figure 2. Illustration of a biphasic association profile. Biosensor data obtained at moderate to high ligate concentrations show association curves that are typically biphasic. The first (fast) and second (slow) phases are shown on this plot, for which the rate constants are $k_{on(1)}=0.09\ s^{-1}$, $k_{on(2)}=0.005\ s^{-1}$, and the magnitudes of the two phases are (A) 200 and (B) 40 arc seconds, respectively.

$$t_{1/2}=\frac{\ln 2}{k_{diss}} \quad (6)$$

Determination of both k_{ass} and k_{diss} allows calculation of the dissociation equilibrium constant, K_D, from Equation 1.

The dissociation equilibrium constant, K_D, can also be determined from the variation of the equilibrium response R_{eq} with ligate concentration, from Equation 7. R_{max} is the response when the immobilized ligand is saturated with ligate.

$$R=\frac{R_{\max}[L]}{K_\mathrm{D}+[L]} \quad (7)$$

Analysis of data using the equations described here was performed by non-linear regression (Johnson, 1992; Leatherbarrow, 1990; Motulsky, 1992; O'Shannessy *et al*., 1993) using the FASTfit software package supplied with the IAsys instrument.

Results

Kinetic analysis of CI2 binding to immobilized chymotrypsin

Association data derived from the biosensor for differing concentrations of CI-2 binding to immobilized chymotrypsin are shown in Figure 3. These data were fitted to equations containing either one (Equation 2) or two (Equation 3) exponential terms also termed monophasic and biphasic equations, respectively. Figure 4a shows the best fit using Equation 2 to the binding data performed at a CI-2

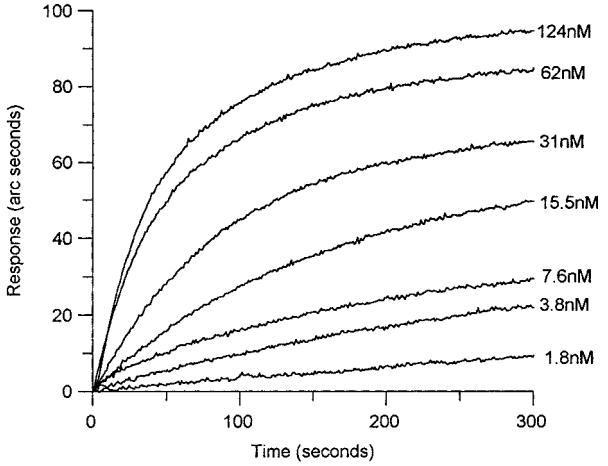

Figure 3. Overlay of association data for CI-2 binding to chymotrypsin immobilized to CMD. The values on the graph show the concentration of CI-2 in the cuvette binding to 437 arc seconds of immobilized ligand.

concentration of 124 nM and Figure 4b shows the best fit of the same experimental data using Equation 3. Figure 4c shows the fit using Equation 2 to experimental data obtained from the binding of 15 nM CI-2. In each case a residual error plot is also shown, illustrating the difference between fitted and experimental values. These figures reveal the effect of ligate concentration upon the association data. At low CI-2 concentrations (<15 nM) the data are fitted well to the expected monophasic equation. However, for data at higher concentrations the monophasic fit is poor with high, systematic residual errors. At these higher concentrations a better description of the data is obtained with a biphasic equation resulting in low, random residual errors, consistent with our previous findings for the binding of tumor necrosis factor (TNF) to an immobilized TNF antibody (Edwards *et al.*, 1995).

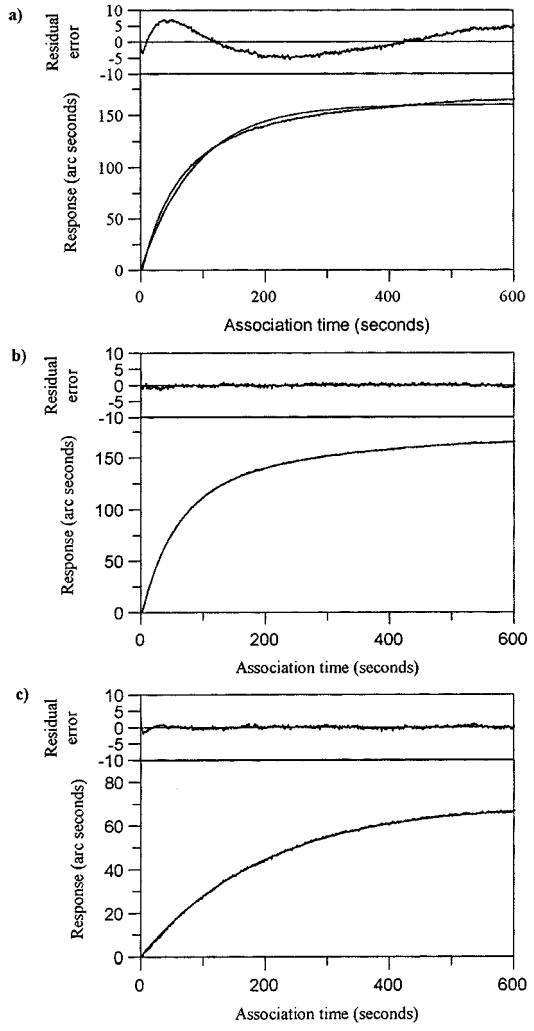

Figure 4. Binding of CI-2 to 977 arc seconds of chymotrypsin immobilized to a CMD cuvette. (a) 124 nM CI-2, single exponential fit. (b) 124 nM CI-2, double exponential fit. (c) 15 nM CI-2, single exponential fit.

Effect of ligand loading upon the association rate constant

Chymotrypsin was immobilized at a variety of concentrations to achieve a range of ligand loadings within the CMD matrix, as shown in Figure 5. A range of immobilization responses from 333 arc seconds to 1110 arc seconds was achieved with a chymotrypsin solution concentration range of 2–2500 μg/ml. The immobilization response resembles a saturation curve, with a plateau being reached when the chymotrypsin solution is around 500 μg/ml or greater.

The binding of CI-2 was measured using a range of CMD surfaces having differing chymotrypsin loadings. For each, the CI-2 was allowed to bind at concentrations ranging from 1.8 nM to 124 nM followed by a regeneration stage after each binding. All association curves were fitted to both single and double exponential equations.

A plot of apparent association rate constant versus ligate concentration was used to determine the k_{ass} as described by Equation 4. At higher ligate concentrations (greater than 15 nM), where the data are not fitted well by a single exponential function, the more rapid rate constant ($k_{on(2)}$) from fitting to an equation containing two exponential functions was taken as the association rate; below 15 nM,

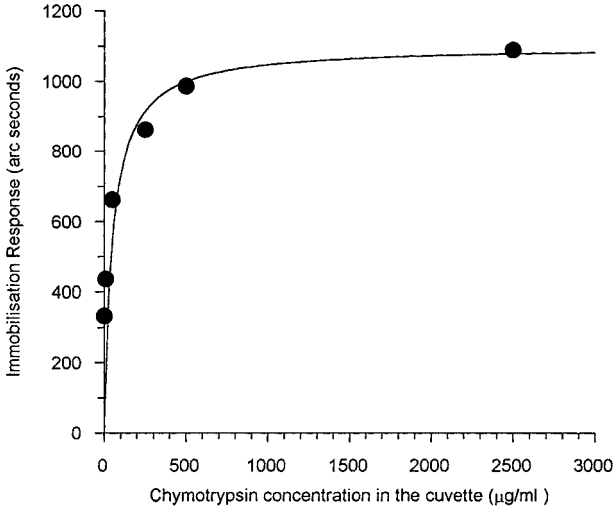

Figure 5. Amount of chymotrypsin immobilized within the CMD matrix measured as biosensor response in arc seconds as a function of the initial chymotrypsin concentration.

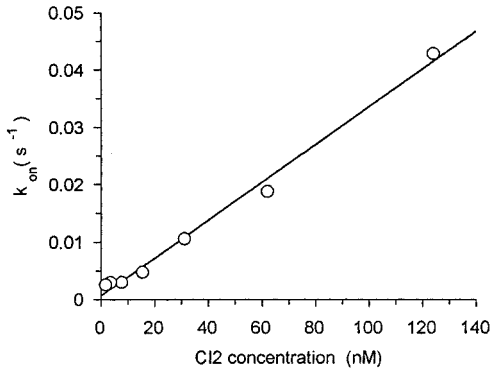

Figure 6. Plot of pseudofirst-order rate constant from curve fitting of CI-2 binding data against the relevant CI-2 concentration.

where the data are fitted well by a single exponential function, the rate constant from such an analysis was used directly. The result of such a plot is illustrated in Figure 6. Figure 7a shows the effect that ligand loading has on the derived association rate constants. High ligand loadings are found to be associated with lower measured association rates compared to those obtained at lower loadings. In the case of CI-2 interacting with immobilized chymotrypsin the association rate reaches a plateau value at loadings of around 600 arc seconds and below, which corresponds to an initial chymotrypsin concentration of lower than 60 μg/ml.

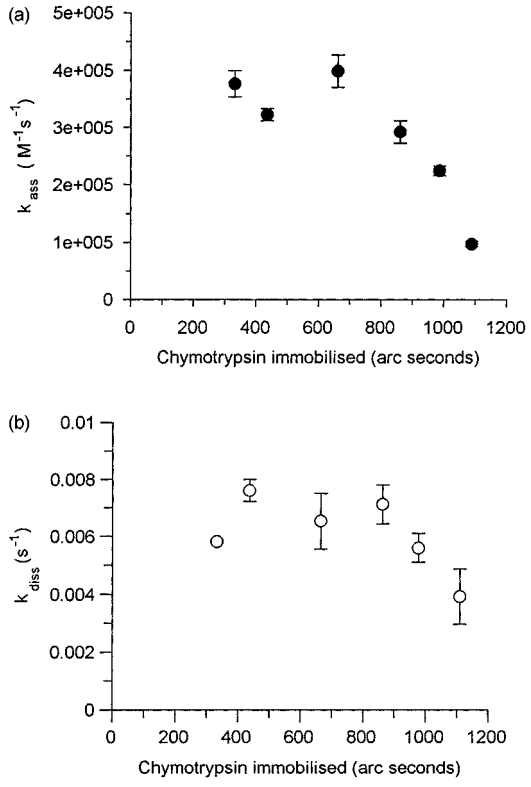

Figure 7. (a) Effect of ligand loading upon the rate of association of CI-2 with chymotrypsin. The rate constants were estimated in duplicate at each ligate concentration. (b) Effect of ligand loading upon the rate of dissociation of CI-2 from immobilized chymotrypsin. The values are the means of the dissociation rate constants determined from three different CI-2 concentrations (124, 64, 32 nM) in duplicate (i.e. n=6 for each immobilization loading).

Effect of ligand loading on dissociation rate constant

The dissociation rate constant of the chymotrypsin-CI-2 complex was determined from application of Equation 5 to the dissociation region of the biosensor profile (Figure 1). With the exception of the first 10 s of dissociation data, which was ignored to allow thermal re-equilibration of the buffer, the whole dissociation region was used (290 s). The variation of k_{diss} with ligand loading is shown in Figure 7b. In the range studied in these experiments, the measured dissociation rate constant was found to be unaffected by the ligand loading up to a loading of 800 arc seconds with a rate of $7\times10^{-3}\,s^{-1}$ ($t_{1/2}$=99 s). Above this loading the value is observed to decrease to $4\times10^{-3}\,s^{-1}$ ($t_{1/2}$=173 s).

Effect of ligand loading on the directly determined dissociation constant

The equilibrium dissociation constant, K_D was calculated directly by the application of Equation 8 to plots of equilibrium response, determined from extrapolation of non-linear regression analysis, against CI-2 concentration as shown in Figure 8. The K_D values obtained at differing chymotrypsin loadings are plotted in Figure 9. The value decreases with decreasing chymotrypsin loading from approximately 42 nM at the highest loadings to 3 nM for the lowest ligand loadings.

Effect of ligand loading upon the extents obtained from curve fitting

The extents from biphasic curve fitting for CI-2 concentrations of 32 nM and 124 nM were determined using the FASTfit software. Figure 10 shows the extent of the second phase (B in Equation 3 and Figure 2) as a percentage of the

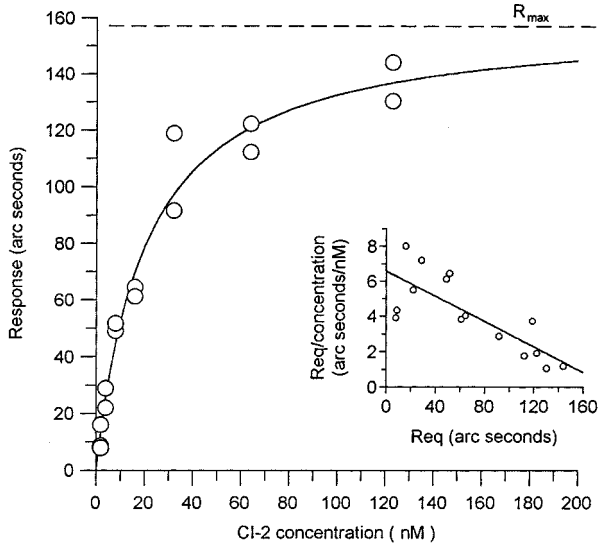

Figure 8. Typical plot of equilibrium response of CI-2 binding to immobilized chymotrypsin. The solid line shows the best fit curve to the data, and a Scatchard plot of the same data is inset. For this plot the amount of immobilized chymotrypsin was 976 arc seconds, and the calculated K_D value is 20 nM.

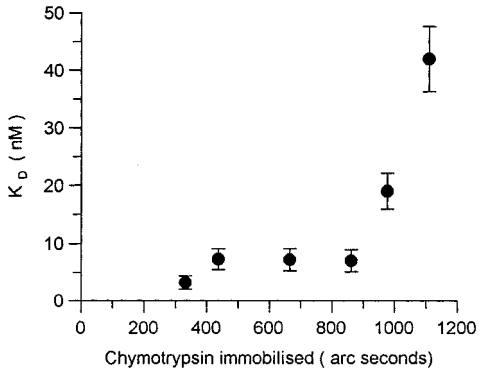

Figure 9. Effect of chymotrypsin loading within the CMD matrix upon the apparent value of K_D directly determined from plots such as Figure 8 for CI-2 binding.

total extent (A+B) against the response arising from differing chymotrypsin loadings at the higher CI-2 concentration of 124 nM. The percentage extent for the lower CI-2 concentration is constant at around 40% and at this lower CI-2 concentration largely unaffected by the loading (data not shown). In contrast, the contribution of the second phase to the total extent at a CI-2 concentration of 124 nM increases with increasing chymotrypsin loading from a value of around 40% at the lower immobilization responses to 90% at the highest loading.

Discussion

The interaction of CI-2 with immobilized chymotrypsin at concentrations above 15 nM fails to be adequately described by equations having a single exponential function (Equation 3, Figure 4a). A better fit to the data is achieved by the incorporation of a second exponential term (Equation 4, Figure 4b). Several publications have highlighted this deviation of the experimental data from that expected for bimolecular interactions in solution (O'Shannessey *et al.*, 1993; Zeder-Lutz *et al.*, 1993; Felder *et al.*, 1993; Corr *et al.*, 1994; Edwards *et al.*, 1995; George *et al.*, 1995). It has been proposed that this phenomenon may be due to, among other reasons, steric hindrance caused by ligate binding, a conformational change in either ligand or ligate upon

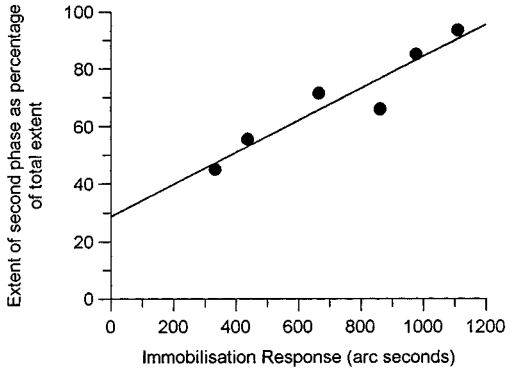

Figure 10. Variation in the contribution of the extent of the slow association phase as a percentage of the total response using cuvettes with varying amounts of immobilized chymotrypsin. For this comparison the concentration of CI-2 used for the association profile was 124 nM.

binding, heterogeneity of immobilized ligand, or multivalency of ligand or ligate. CI-2 binds to chymotrypsin to form a 1:1 complex, and so in this case the biphasic nature of the association plots cannot be due to multivalency. We have previously shown that an important cause of this phenomenon is the steric hindrance caused by ligate binding within a crowded hydrogel surface layer (Edwards *et al.*, 1995), and this effect is demonstrated again for the binding of CI-2. At the higher CI-2 concentrations, binding to the readily accessible ligand will result in the first, rapid rate constant ($k_{on(1)}$) which is comparable to that found in solution. The second slower rate ($k_{on(2)}$) arises from the restricted access to some of the immobilized ligand and so is specific to the biosensor experiment. We find that the proportion of the instrument response due to this second, slower phase increases with ligand loading, particularly at high ligate concentrations. Figure 10 shows that the contribution of the second phase to the overall extent at a ligate concentration of 124 nM is greatly dependent upon ligand loading, and varies from an extrapolated 30% of the total response at zero ligand to 90% at the highest loading of 1110 arc seconds (2500 μg/ml chymotrypsin in the cuvette). This effect is consistent with our proposal that the slow second phase arises from steric hindrance causing restricted access within the dextran matrix (Edwards *et al.*, 1995), as high ligand loading would be expected to exacerbate the effect in precisely the manner found.

A predicted consequence of the effects of steric hindrance as described here is that differing ligand loadings will affect the association and dissociation data derived from the biosensor. In order to examine this, a series of experiments were performed that monitored the interaction between chymotrypsin and CI-2 using varying loadings of immobilized chymotrypsin. The effect on the derived association rate constant is shown in Figure 7a. It is found that at the lower ligand concentrations a plateau region is obtained with an apparent association constant of approximately $4\times10^5\ \text{M}^{-1}\,\text{s}^{-1}$. As the ligand loading of the hydrogel matrix is increased, the apparent association rate is reduced by a factor of four. Analysis of dissociation data showed that this rate is unaffected by ligand loading until a loading of approximately 800 arcsec is achieved. At higher loadings the dissociation rate constant decreases, possibly due to rebinding of the ligate to immobilized ligand within the dextran matrix. It is interesting to note that the rate determined from exponential fitting of the actual dissociation data is six times faster than that determined from the intercept of plots such as Figure 6. It is well known that the intercept of such plots is prone to inaccuracies due to extrapolation to a value close to zero, however, this seems unlikely to account for the difference observed here, and the reason for the discrepancy is unknown at present.

Given the effect on the association rate constants and to a lesser extent on the dissociation rate constants, it is not surprising that ligand loading also has an effect upon the value of K_D. For the chymotrypsin/CI-2 interaction the K_D value decreases (i.e. a higher affinity) with decreasing loadings as illustrated in Figure 9. At low loadings the value becomes constant, at 6.2 ± 2.0 nM. The K_D value determined from the ratio of dissociation to association rate constants (Equation 6) is found to be 15.7 ± 3.4 nM. These two independent methods of calculating the K_D value give

similar, although not identical, values. It seems likely that the discrepancy between these methods is a more realistic indication of the experimental errors in this analysis than the statistics derived from the regression analyses of plots such as Figure 6 or non-linear regression analyses of plots such as Figure 8 alone.

The chymotrypsin/CI-2 system has been well characterized by direct measurements of enzyme kinetics using a chromogenic substrate (Longstaff *et al*., 1990). A comparison of these association rates with those from the biosensor show those measured by the biosensor to be approximately seven-fold lower. However, the measured dissociation rate constants are very similar. Association rate constants derived from biosensor studies using hydrogel surfaces are frequently found to be lower than those observed in solution, at least partly because the diffusion coefficient of the immobilized ligand is lower than that in solution (Karlsson *et al*., 1994). A further possible cause for the lower association rate constants for experiments involving binding to a surface is mass-transport limitations. However, this seems unlikely for two reasons. First, the association rate constant for this system is less than values obtained for other interacting biomolecules that have been successfully characterized using the same biosensor technology. Second, such mass-transport effects would be accompanied by sigmoidal association profiles, and the data obtained for this system did not demonstrate any such effects.

Conclusion

The determination of kinetic constants using optical biosensor technology is becoming more common given the advantages that such techniques offer over more conventional methods. However, care must be taken in experimental design when deciding on the ligand immobilization levels and ligate concentration range. The level of ligand immobilization is found to have a pronounced influence on the apparent values of kinetic constants derived from a biosensor experiment. Low immobilization levels are essential when determining kinetic constants in order to minimize steric interference with ligate binding. Failure to do so may result in an under-estimate of the association rate constant with a subsequent over-estimation of the dissociation equilibrium constant, K_D compared to that in solution.

References

Bondeson, K., Frostel, Å., Katlsson, R., Fägerstam, L. and Magnusson, G. (1993). *Anal. Biochem.* **214**, 245–251.

Buckle, P. E., Davies, R. J., Kinning, T., Yeung, D., Edwards, P. R., Pollard-Knight, D. and Lowe, C. R. (1993). *Biosensors and Bioelectronics* **8**, 355–363.

Corr, M., Slanetz, A. E., Boyd, L. F., Jelonek, M. T., Khilko, S., Al-Ramadi, B. K., Kim, Y. S., Maher, S. E., Bothwell, A. L. M. and Marguiles, D. H. (1994). *Science* **265**, 946–949.

Cush, R., Cronin, J. M., Stewart, W. J., Maule, C. H., Molloy, J. and Goddard, N. J. (1993). *Biosensors and Bioelectronics* **8**, 347–353.

Davies, R. J., Edwards, P. R., Watts, H.J., Lowe, C. R., Buckle, P. E., Yeung, D., Kinning, T. M. and Pollard-Knight, D. V. (1994). In *Techniques in Protein Chemistry V,* pp. 285–292. Academic Press, London, UK.

Dubs, M.-C., Altschuh, D., and van Regenmortel, M. H. V. (1991). *Immunol. Letts.* **31**, 59–64.

Edwards, P. R., Gill, A., Pollard-Knight, D. V., Hoare, M., Buckle, P. E., Lowe, P. A. and Leatherbarrow, R. J. (1995). *Anal. Biochem.* **231**, 210–217.

Fägerstam, L. G., Frostell, Å., Karlsson, R., Kullman, M., Larsson, A., Malmqvist, M. and Butt, H. (1990), *J. Mol. Recogn.* **3**, 208–214.

Felder, S., Zhou, M., Hu, P., Urena, J., Ullrich, A., Chaudhuri, M., White, M., Shoelson, S. E. and Schlessinger, J. (1993), *Mol. Cell. Biol.*, **13**, 1449–1455.

George, A. J. T., French, R. R., and Glennie, M. J. (1995). *J. Immunol. Methods.* **183**, 51–63.

Jandu, S. K., Ray, S., Brooks, L. and Leatherbarrow, R. J. (1990). *Biochemistry* **29**, 6264–6269.

Johnson, M. L. (1992). *Anal. Biochem.* **206**, 215–225.

Karlsson, R., Roos, H., Fägerstam, L. and Persson, B. (1994). *Methods: A companion to Methods in Enzymology.* **6**, 99–110.

Kelley, R. F., and O'Connell, M. P. (1993). *Biochemistry* **32**, 6828–6835.

Leatherbarrow, R. J. (1990). *Trends Biol. Sci.* **15**, 455–458.

Longstaff, C., Campbell, A. F. and Fersht, A. R. (1990). *Biochemistry* **29**, 7339–7347.

Mach, H., Volken, D. B., Burke, C. J., Middaugh, C. R., Linhardt, R. J., Fromm, J. R. and Loganathan, D. (1993). *Biochemistry* **32**, 5480–5489.

Malmborg, A. C., Michaëlsson, A., Ohlin, B., Jansson, B. and Borrebaeck, C. A. K. (1992). *Scand. J. Immunol.* **35**, 643–650.

Motulsky, H. J. and Ransnas, L. A. (1987). *FASEB J.* **1**, 365–374.

O'Shannessy, D. J., Brigham-Burke, M., Soneson, K. K., Hensley, P. and Brooks, I. (1993). *Anal. Biochem.* **212**, 457–468.

Stanley, C., Lew, A. M. and Steward, M. W. (1983). *J. Immunol. Methods* **64**, 119.

Tiefenthaler, K. (1993). *Biosensors & Bioelectronics* **8**(7) xxxv–xxxvii.

Watts, H. J., Lowe, C. R. and Pollard-Knight, D. V. (1994). *Anal. Chem.* **66**, 2465–2470.

Zeder-Lutz, G., Altschuh, D., Geysen, H. M., Trifilieff, E., Sommermeyer, G. and van Regenmortel, M. H. V. (1993). *Mol. Immunol.* **30**, 145–155.

